MDPI

Article

Classical Nuclear Motion: Comparison to Approaches with Quantum Mechanical Nuclear Motion

Irmgard Frank

Institute of Physical Chemistry and Electrochemistry, Theoretical Chemistry, Leibniz University of Hannover, Callinstr. 3A, 30167 Hannover, Germany; irmgard.frank@theochem.uni-hannover.de

Abstract: Ab initio molecular dynamics combines a classical description of nuclear motion with a density-functional description of the electronic cloud. This approach nicely describes chemical reactions. A possible conclusion is that a quantum mechanical description of nuclear motion is not needed. Using Occam's razor, this means that, being the simpler approach, classical nuclear motion is preferable. In this paper, it is claimed that nuclear motion is classical, and this hypothesis will be tested in comparison to methods with quantum mechanical nuclear motion. In particular, we apply ab initio molecular dynamics to two photoreactions involving hydrogen. Hydrogen, as the lightest element, is often assumed to show quantum mechanical tunneling. We will see that the classical picture is fully sufficient. The quantum mechanical view leads to phenomena that are difficult to understand, such as the entanglement of nuclear motion. In contrast, it is easy to understand the simple classical picture which assumes that nuclear motion is steady and uniform unless a force is acting. Of course, such a hypothesis must be verified for many systems and phenomena, and this paper is one more step in this direction.

Keywords: Car–Parrinello molecular dynamics; chemical reactions; photoreactions; classical nuclear motion

1. Introduction

What led us to describing nuclear motion classically in simulations of chemical reactions [1–3]. It all started with the famous publication of Car and Parrinello [4]: "Unified Approach for Molecular Dynamics and Density-Functional Theory". In their seminal work, Car and Parrinello started from the Born–Oppenheimer approximation to "separate nuclear and electronic coordinates" [4]. With this understatement, the resulting method is what sometimes is called semiclassical: density functional theory (DFT) for the electrons and a classical treatment for the nuclei (it should be mentioned that the general idea was in the world before; see the Nobel prize lecture of Karplus). While being deterministic, the approach of Car and Parrinello is different from Bohm mechanics, which merely reformulates Schrödinger's theory. Instead of a "guiding equation", as in Bohm's theory, we have simply Newton's equation.

Car and Parrinello constructed an extended Lagrangian and made it possible to use this idea in a working code. They developed a numerically extremely successful concept: density functionals at the generalized gradient approximation (GGA) level/pseudopotentials for the inner electrons/periodic boundary conditions/plane waves for the valence electrons/Car–Parrinello equations for electronic motion. This approach is efficient for several reasons: 1. The use of plane waves makes it possible to perform simulations with changing atomic distances without a basis superposition error and without Pulay forces, that is, we obtain no additional terms by pulling basis functions through space. 2. If huge plane-wave basis sets are used, we are essentially restricted to GGA functionals. Hybrid functionals are too expensive due to the use of Hartree–Fock exchange. 3. Pseudopotentials make the plane-wave basis sets tractable. This results in almost complete basis sets for the valence electrons.

At the start of a Car–Parrinello molecular dynamics (CPMD) simulation, the electronic structure is computed using density functional theory. During the simulation, it is propagated using the Car–Parrinello equations. These equations include an additional term which contains the forces on the electronic cloud, that is, the second derivatives of the orbitals multiplied by a fictitious electron mass. It is unpleasant to need such a parameter as the fictitious electron mass, but this parameter can be varied over two orders of magnitude without a strong change. By setting it to about 400–500 atomic units instead of 1 atomic unit, it is possible to save CPU time. The result works excellently. This may be explained by the beauty of the Car–Parrinello equations: we have second derivatives for both space and time. It is a purely deterministic approach that can be solved numerically, time step by time step, using Equation (5a,b) in Ref. [4]. Time steps are introduced during which the forces can be assumed as constant. They have typical values of about 0.1 fs. Normally, this leads to stable dynamics. The implementation of the Car–Parrinello equations is not easy; hence, not so many implementations exist. The most famous is the CPMD code written by Hutter et al. [5], which is extremely well parallelized and is also very user-friendly. The CPMD code also contains an implementation of what is called Born–Oppenheimer dynamics (BOMD), namely, molecular dynamics with full optimization of the electronic wave function in every time step instead of a CP molecular dynamics. Both BOMD and CPMD are summarized as ab initio molecular dynamics (AIMD). BOMD is almost one order of magnitude slower than CPMD, depending on the time step chosen. Since in BOMD simulations the motion of the electrons does not have to be resolved, a larger time step (0.1–0.5 fs) than in CPMD simulations (0.05–0.1 fs) may be used. Using a too-large time step leads to a drift of the total energy (see Supplementary Material, Figures S1–S5).

The approach to compute only the points that are reached during dynamics, instead of calculating a complete potential energy surface, is called "on the fly" simulations. Two simulations starting from the same initial conditions will always lead to the same result. Slightly changing the initial conditions can lead to different products, that is, we have deterministic chaos but no quantum chaos. Since the velocities of the atoms are Maxwell–Boltzmann-distributed, there is no classically forbidden region [3]. We do not have to do anything to achieve this distribution. It develops automatically in a molecular dynamics run as it is the most likely distribution. The fastest parts of a molecular system may undergo chemical reactions.

One more point that should be mentioned is the kinetic isotope effect: in contrast to the static isotope effect, it can normally be measured. When using Newton dynamics, this is explained by the fact that the force depends on the mass, F = m a. In contrast, static isotope effects that depend on the zero-point energy cannot be observed. While there is a lot of zero-point energy in the electronic wave function of every atom due to the $1/r$ potential, there is no zero-point energy in nuclear motion. This facilitates the understanding of matter at low energies: near-zero-Kelvin nuclei hardly move, while the electrons form a static cloud that cannot be compressed much stronger.

In the present paper, I will compare CPMD and BOMD results, as obtained with the CPMD code, to the pioneering work of Marx [6–9], Domcke [10–13], Hammes-Schiffer [14], Martinez [15,16], and coworkers, certainly ignoring many others (for a review, see, for example, Ref. [11]). It is the experience from these excellent studies that leads to the thought that a quantum mechanical description of nuclear motion is not needed. For the excited states I will use restricted open-shell Kohn–Sham (ROKS) calculations [17]. Hereby, ROKS is merely an approach that solves the electronic structure problem for excited states self-consistently with minimum computational effort at the DFT level of accuracy. An interesting feature of ROKS is that, as a single-configuration method, it is diabatic. We use the single electronic configuration that describes a pure HOMO–LUMO transition. During a chemical reaction, for example, a dissociation, this configuration may become the open-shell ground state. Alternatives are real-time TDDFT methods [18–22], which use time-dependent DFT in their original meaning, without using perturbation theory. This field is still in development. Of course, time-dependent DFT also describes the electronic

wave function only. Similar to other quantum chemical excited-state methods, it can be combined with classical or quantum mechanical nuclear motion.

2. Methods

Using the CPMD code, ab initio molecular dynamics simulations [4,5,23] were performed in the NVE ensemble using the Becke–Lee–Yang–Parr (BLYP) functional in connection with the Grimme dispersion correction [24]. The wave function was optimized in every time step ("Born–Oppenheimer molecular dynamics"). For comparison, some calculations were performed with Car–Parrinello molecular dynamics. The time step was chosen as 5 a.u. (0.1209 fs). This time step is relatively small for BOMD simulations and was chosen in order to describe the excited state as accurately as possible. Troullier–Martins pseudopotentials, as optimized for the BLYP functional, were employed for describing the core electrons [25,26]. The plane-wave cutoff, which determines the size of the basis set, was set to 70.0 Rydberg. This corresponds to a very large basis set. In the case of the phenol photodissociation, the simulation cell size was $14 \times 14 \times 14$ a.u.^{3} ($7.4 \times 7.4 \times 7.4$ Angstrom). For the orbital plots, a cell size of $18 \times 18 \times 18$ a.u.^{3} ($9.5 \times 9.5 \times 9.5$ Angstrom) was chosen in order to account for the diffuse character of the LUMO in the Franck–Condon region. After geometry optimization, an equilibration in the ground state was performed, with initial temperatures ranging from 0 to 2000 K. During the equilibration, half of this initial kinetic energy is converted into potential energy, leading to temperatures that are only half as high. The kinetic energy distribution was chosen in this way in order to model a Maxwell–Boltzmann distribution, which permits high energies of single particles. In the ground state, the molecules are stable under these conditions on the picosecond timescale. After equilibration, the system was placed vertically into the excited state by changing the occupation pattern (restricted open-shell Kohn–Sham, ROKS [17]) while keeping the ground-state velocities.

The same protocol was used for bipyridyl systems, except that the simulation cell was always kept at $18 \times 18 \times 18$ a.u.^{3} ($9.5 \times 9.5 \times 9.5$ Angstrom). The initial kinetic energies were varied between 600 and 2400 K.

For comparison, CPMD simulations were performed (see the Supplementary Material). The time step was chosen as 2 a.u. (0.048 fs), and the fictitious electron mass as 200 a.u.

3. Results

3.1. Wave Packets and Alternatives

The Schrödinger equation for any system composed of atoms reads:

$$\hat{H}_{total}\Psi = E_{total}\Psi \tag{1}$$

$$\hat{H}_{total} = \hat{T}_{nuc} + \hat{T}_{el} + \hat{V}_{nuc-nuc} + \hat{V}_{nuc-el} + \hat{V}_{el-el} \tag{2}$$

The Hamilton operator contains all kinetic and potential energy terms: the kinetic energies of nuclei and electrons plus the nuclear–nuclear interactions, the nuclear–electronic interactions, and the electronic–electronic interactions. At this point, normally, the Born–Oppenheimer approximation is applied, separating the electronic problem in the electronic Hamilton operator:

$$\hat{H}_{el} = \hat{T}_{el} + \hat{V}_{nuc-el} + \hat{V}_{el-el} \tag{3}$$

Applying density functional theory (or other approximations to the electronic problem) to ground and excited states of a molecular system yields what is known as Born–Oppenheimer surfaces or also potential energy surfaces. For covalent interactions, Morse potentials are obtained. This, however, works only if the nuclear–nuclear interaction is added to the energy computed for the electronic Hamiltonian. This is no small correction: if the nuclear–nuclear interaction is omitted, the nuclei collapse to a distance of zero Angstrom. Without the nuclear repulsion, the minimum of the Morse potential, which keeps the nuclei at a distance, disappears. Hence, the total energy in a normal quantum

chemical calculation contains the kinetic energy of the electrons, the electron–electron interaction, the electron–nuclear interaction, and the nuclear–nuclear interaction:

$$\hat{H}_{QC} = \hat{T}_{el} + \hat{V}_{nuc-nuc} + \hat{V}_{nuc-el} + \hat{V}_{el-el} \tag{4}$$

The only term missing is the kinetic energy of the nuclei. This corresponds to the situation at zero Kelvin. Hence, normal quantum chemical calculations are performed at zero Kelvin. This changes if ab initio molecular dynamics is employed: then, the kinetic energy of the nuclei is replaced by the classical term. The structure or motion of the nuclei does not play any role in quantum chemical calculations. By good luck, the structural differences between zero Kelvin and room temperature are normally small in molecular systems. Hence, we know how to compute potential energy surfaces: not by introducing a product ansatz and a separation of variables, but by setting the temperature of the nuclear system to zero. It is consistent to treat the nuclei as classical particles right from the beginning as practiced in AIMD simulations. As a result, we have a wave function for the electrons only, no product ansatz, and no separation of variables. All five energy terms act on this electronic wave function:

$$\hat{H}_{AIMD}\Psi_{el} = (\hat{T}_{nuc,classical} + \hat{T}_{el} + \hat{V}_{nuc-nuc} + \hat{V}_{nuc-el} + \hat{V}_{el-el})\Psi_{el} = E_{AIMD}\Psi_{el} \tag{5}$$

In the SCF calculation, only the three of them which are contained in $\hat{H}_{el}$ matter. The two remaining energy terms are added after the SCF or, in a CPMD simulation, once in every time step. The nuclear–nuclear interaction is simply the electrostatic interaction of classical point particles.

Taking derivatives of the total energy expression $\hat{H}_{AIMD}$ with respect to the classical nuclei, we obtain the following classical equation for the nuclei:

$$M_I \ddot{\underline{R}}_I = -\frac{\partial}{\partial \underline{R}_I} E_{QC} \tag{6}$$

Capital letters are used for the nuclei. In addition, this equation for the nuclei contains all five terms: on the left side, we have the derivative of the classical kinetic energy, that is, the accelerations or forces; on the right side, we have the derivative of E_{QC} which contains the remaining four terms.

As is known from experiments, nuclei have a certain size, which is in the region of a few femtometers. There is no theoretical approach which would yield this size in a reliable way, such as the electronic Schrödinger equation reliably yielding the extension of the electronic cloud. We can explain the periodic system, but not the isotope chart. Within the isotope chart, the density of the nuclei is almost constant; hence, they do not become smaller with increasing mass. A naive application of the deBroglie theory of matter waves would yield a wrong result. Similar to any massive object, the mass, and not the size, of a particle determines the motion of its center of mass.

Let us return to the potential energy surfaces. It is a wide and well-established field of research to compute these surfaces with standard quantum chemical methods and, in a second step, to model the nuclear situation using wave packet approaches. However, these wave packets are too large, by several orders of magnitude, to be related to the structure of a nucleus. Nuclear wave packets may spread and recombine, which, however, is not interpreted as nuclear fission or fusion. It is, rather, assumed that the nuclear wave function is smeared out and that this can be healed by a measurement, eventually leading to different chemical products; however, such a smeared nuclear wave function (or, rather, its density) is never observed in experiment. There is no reason to give up the Rutherford picture of tiny nuclei, which are larger the heavier the nucleus is. Nowadays, with large computers, it may seem the better alternative to switch to classical many-body theory for nuclear motion instead of investigating wave packets in a few dimensions.

What about photoreactions? In addition, in this context, what about branching at conical intersections? It is certainly true that conical intersections are everywhere [27];

however, they are far less responsible for the outcome of a photoreaction than the dynamics in the Franck–Condon region which may lead the way to different conical intersections [28]. An example is the photochemistry of CH$_3$Cl [2]. Immediately after excitation, the system may decide in which direction to move: either C–Cl dissociation or C–H dissociation. The conical intersections for both reaction paths are reached much later. If, similar to the restricted open-shell Kohn–Sham (ROKS) method [17], a diabatic method is used, the nuclei do not behave strangely at these conical intersections. In the single-configuration ROKS picture, which is diabatic by construction, the nuclei simply accelerate while the system is reaching lower regions of the potential energy surface. They do not branch, nor do they show any other strange behavior at the diabatic crossings. It was also shown for pyrrole that this is sufficient to explain the experiment [29]: there is a shallow minimum near the Franck–Condon region which causes a second reaction channel. This second reaction channel is not due to the motion near the conical intersection, which is reached later.

ROKS yields excited-state gradients in a straightforward way using the Hellmann–Feynman theorem. Nevertheless, one might hope for a more versatile approach if extending this to an adiabatic many-configuration ansatz followed by a nonadiabatic treatment. Surface hopping does not solve the problem [13]. More interesting is the use of a diabatization which, however, is not uniquely defined [30]. When making a comparison between wave-packet and on-the-fly methods, the drawbacks of the on-the-fly methods must also be emphasized. Of course, the diabatic ROKS method also has its shortcomings. In particular, there is presently no convincing implementation which would allow for the use of hybrid functionals. As a result, we typically obtain a vertical excitation energy which is too low by about 0.6 eV, which we compensate by starting with higher kinetic energies. In addition, similar to the case for any excited-state self-consistent field calculation, convergence is much worse than for the ground state, and sometimes jumps in the total energy are observed. Finally it is not possible at the moment to combine Car–Parrinello molecular dynamics and ROKS. We are restricted to Born–Oppenheimer molecular dynamics simulations. Yet, this does not affect nuclear motion, and the classical picture of nuclear motion survives.

In the present study, we apply ROKS/BLYP to the photoreaction of phenol, which was studied before by Domcke and coworkers [10,12,31]. While in these wave-packet calculations the average O–H distance reaches 3 Angstrom within 30 fs, we observe only partial dissociation. In most simulations (7 out of 10), we observe no photoreaction at all within 1.2 ps of simulation time. In the remaining cases, we observe the dissociation connected to the transformation of the LUMO to a 1s orbital, while the HOMO hardly changes shape (Figures 1 and 2). The transformation is mostly smooth, but there is a problem with the SCF about 0.02 ps after the excitation. The wave function suddenly changes sign, which is accompanied by a slight jump in energy (see the Supplementary Material, Figure S6). This is one of the disadvantages of Born–Oppenheimer molecular dynamics compared to Car–Parrinello molecular dynamics: such sudden changes in an SCF calculation are numerically possible. The same applies to the slight slope of the total energy. In addition, here, Car–Parrinello molecular dynamics would be superior, even if we use a very small time step (0.1 fs) in the Born–Oppenheimer dynamics simulations.

The reaction path observed consists mainly of the dissociation of the O–H bond. The LUMO of phenol is transformed into the 1s orbital of the resulting hydrogen atom. As can be seen in Figure 2, after 48 fs, the bond cleavage is supported by an interaction with a neighboring hydrogen atom. With all the drawbacks of ROKS, we obtain a very clear and convincing picture of the development of the electronic structure during this photoreaction. The picture obtained by a wave-packet description [10] is also convincing. While in the classical picture the observation of different outcomes is due to the dynamics in the Franck–Condon region, the quantum mechanical picture attributes the branching to the motion through conical intersections. One might mention, however, that in the quantum mechanical description, the nuclear probability density of the product state is smeared over several Angstrom, which is not necessarily a realistic picture.
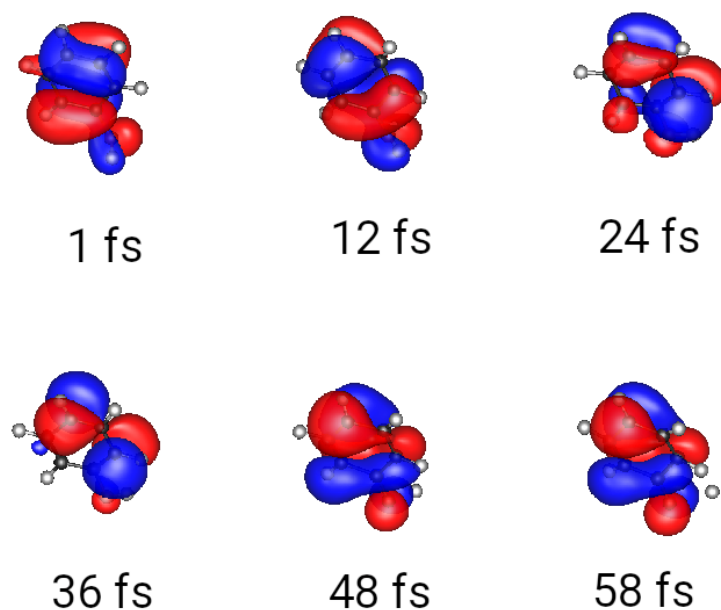
Figure 1. HOMO of phenol during the photoreaction (ROKS simulation). Apart from a rapid change of sign between 12 and 24 fs, not much happens to the electronic structure. A hydrogen atom is expelled at the end of the simulation (at the right side of the molecule).
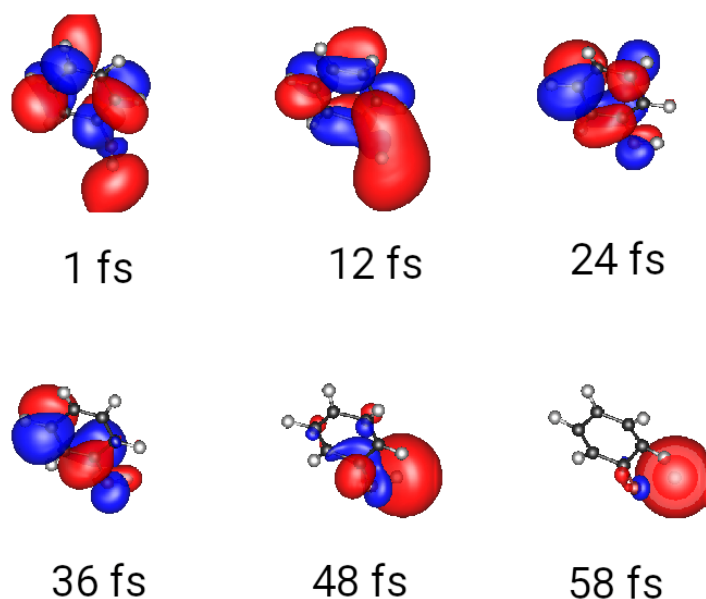

Figure 2. LUMO of phenol during the photoreaction (ROKS simulation). The motion starts from a π^* orbital which has already an antibinding interaction concerning the O–H bond. The elongation of this bond leads to the formation of the 1s orbital of the dissociating hydrogen atom.

3.2. Multiple Spawning

Martinez and coworkers developed, very early, a quantum mechanical implementation of nuclear motion. With multiple spawning, the situation in nonadiabatic regions, e.g., near a conical intersection, is described [15]. The authors already presented, in 1998, an impressive application to the photoisomerization of retinal in bacteriorhodopsin [32]. A related problem, namely, the photoisomerization of retinal in bovine rhodopsin, was studied with ROKS/BLYP using a QM/MM approach in order to model the protein environment [33]. The ROKS study, using excited-state self-consistent field (SCF) theory, produced the particularly nice result that of all double bonds in retinal which could isomerize, only the C_{11}–C_{12} bond rotates upon excitation. This is due to the shape of

the binding pocket and to the location of the counterion. However, to be precise concerning all advantages and disadvantages, it must be mentioned that a higher temperature had to be applied to compensate for the ROKS/BLYP redshift. The result is one of still very few unconstrained QM/MM simulations showing a chemical reaction in a protein on the fly. In the multiple spawning calculations, the shape of the quantum mechanical nuclei is strongly determined by Gaussian basis functions, and care must be taken not to obtain complete delocalization. Again, the conceptionally simpler (but computationally way more expensive) diabatic AIMD model with classical nuclear motion has some advantages. In any case, also for protein chemistry, we find no reason to assume quantum effects in nuclear motion. The experience from QM/MM calculations, rather, leads to the conclusion that nuclear motion may be described in the same way for both the QM and the MM parts of the system.

3.3. Path Integrals

A concept based on the work of Feynman is the use of path integrals. In the application to molecular problems [6–9], multiple pathways are computed during a complete on-the-fly simulation. Typically, ground state situations were treated. The implementation of path integrals in the CPMD code made it possible to simulate fluxional molecules at this high theoretical level; however, comparison to experiment does not prove at all that a quantum description of nuclear motion is necessary. Temperature has a qualitatively similar effect. More recently, it was shown that path-integral MD works far worse when applied to the simulation of chemical reactions [2]. For example, in a dissociation reaction, the nuclear clouds of both fragments stay entangled. It is not clear by what mechanism, and at what point in time, that this entangled result could possibly be transformed again into reasonable molecules. Feynman's view of quantum mechanics was based on thought experiments [34]. It may be applied fruitfully in high-energy situations, but not in quantum chemistry. Classical on-the-fly computations on large computers lead to a different picture.

3.4. Full Treatment

An important step towards a full treatment of both electronic and nuclear structure was made by Hammes–Schiffer and coworkers [14,35,36]. In their nuclear-electronic orbital (NEO) method, the authors do not make use of the Born–Oppenheimer separation, but solve the complete problem straightforwardly. In numerical applications, however, only the nuclei of the hydrogen atoms are selected for a quantum mechanical treatment. The authors succeeded in programming analytic excited-state gradients, which facilitated the computation of optimized geometries. For the description of the electronically excited states, they used time-dependent density functional theory (TDDFT), respectively, the combination NEO-TDDFT.

While this should be a powerful approach, it is observed that the nuclei are smeared out over a distance that is much larger than 1 fm. It might be the choice of the Gaussian basis set which keeps them at the size observed. The quantum mechanical treatment of all the nuclei is computationally expensive. Yet, there might be yet another reason for not computing all nuclei quantum-mechanically: if all nuclei are treated in this way, there will be no external potential left, and both the electronic and the nuclear densities will be smeared out. A critical test for the method, which does not cost too much CPU time, might be the fully quantum mechanical simulation of hydrogen formation from two hydrogen atoms, ideally using an unbiased plane-wave basis set [2].

In order to compare, we performed ROKS simulations for the 2,2′-bipyridine, [2,2′-bipyridyl]-3-ol and [2,2′-bipyridyl]-3,3′-diol systems. The latter two substances were investigated by Hammes–Schiffer and coworkers. For bipyridyl-diol, we find an immediate hydrogen transfer from the OH groups to the nitrogen atom. Movies of the two singly occupied orbitals are added in the Supplementary Material. The mechanism corresponds to an excited-state intramolecular proton transfer (ESIPT). The two proton transfers are almost simultaneous (Figure 3). While this reaction is fast, we observe no rotation about the central

carbon–carbon bond [36]. This is no surprise: the lowest unoccupied molecular orbital (LUMO), which is populated upon excitation, exhibits a binding interaction for the central carbon–carbon bond (Figure 4). The same is true for bipyridine and bipyridyl-ol (Figure 5). In the ROKS simulations, we observe no motion that would explain radiationless decay. Near the excited-state minimum, we place the system back to the ground-state surface. This is connected with a jump in energy (see the Supplementary Material, Figures S7 and S8). This jump is due to the fact that we converge the wave function in every time step. A more realistic picture of the electronic motion near the state crossing could be obtained if we could use a CPMD-like approach, with a steady and continuous motion of all parts of the system, instead of BOMD, with full convergence of the orbitals. This does not affect nuclear motion; the ESIPT is described correctly.
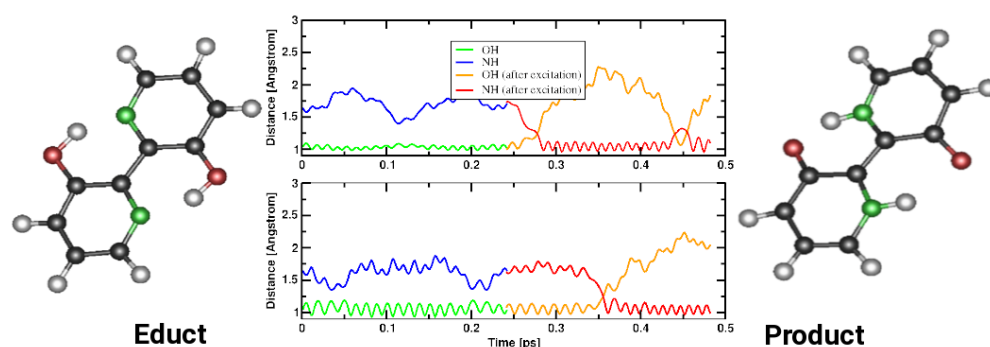

Figure 3. Photoreaction of [2,2′-bipyridyl]-3,3′-diol, ROKS simulation. Upper and lower panel: reaction of the two OH groups, respectively. The isomerization events, which are characterized by a crossing of the orange and red curves, are not exactly simultaneous, but follow closely one after the other. Color code of educt and product plots: white: hydrogen, black: carbon, green: nitrogen, red: oxygen.
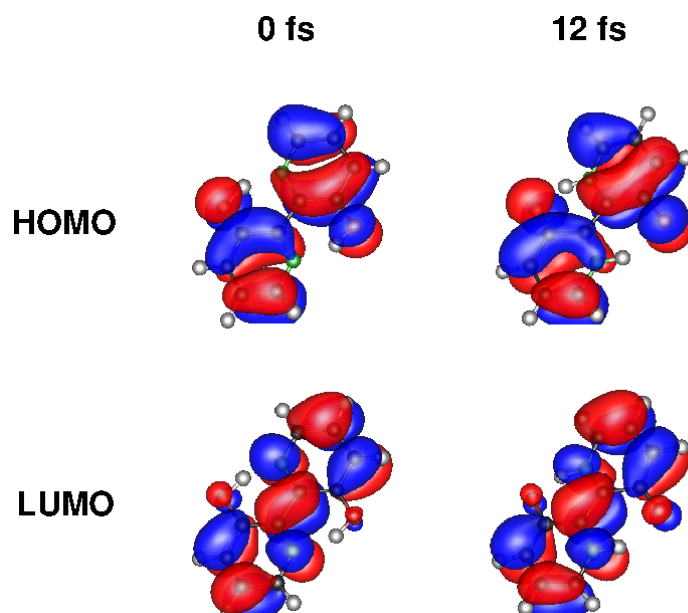

Figure 4. HOMO and LUMO of [2,2′-bipyridyl]-3,3′-diol before and after the photoreaction. The central carbon–carbon bond is strengthened in the excited state and adopts double bond character.
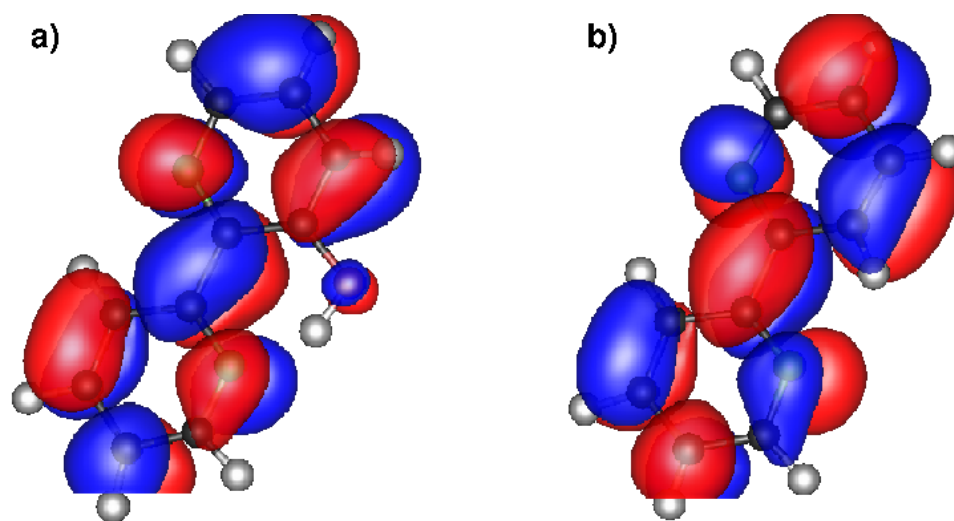
Figure 5. (**a**) LUMO of [2,2'-bipyridyl]-3-ol; (**b**) LUMO of bipyridine. The LUMOs resemble the LUMO of bipyridyl-diol. Upon occupation of this orbital, the central carbon–carbon bond is strengthened. This prevents a rotation.

4. Discussion

It is the state of the art to compute the electronic structure at the DFT level and nuclear motion classically in an on-the-fly approach. The basis of this picture is a model that is in agreement with the Rutherford atom model concerning the nuclei, while the electronic structure is computed using the Schrödinger equation: tiny, positively charged nuclei are surrounded by a negatively charged electronic cloud. In contrast to the electrons, the nuclei (C, H, O, N, etc.) can be discriminated. This model ignores the possibility of nuclear fusion and fission, i.e., the nuclei in our picture are perfectly stable. Obviously, we make an approximation and we investigate if this approximation is superior to the quantum mechanical picture of nuclear motion. In a classical description, there is no zero-point energy in nuclear motion. This represents no problem since, due to the 1/r potential, our bound electrons have infinite zero-point energy, which is more than enough. Very obviously, the approach we use (Schrödinger equation for the electronic structure, Newton dynamics for the nuclear motion) works for bound electrons only and is an approximation to a more general field theory. It is not unlikely that such a more general field theory is numerically intractable for the problems we are investigating. In other words, chemistry gives us little information about the inner structure of a nucleus.

The photoreactions investigated in this study involve the breaking and formation of bonds with hydrogen atoms. There is no reason to assume that hydrogen behaves less classically than other atoms. ROKS is an approximate method that extends the basis of density functional theory to an excited-state SCF with an excited-state gradient. In all practical implementations, ROKS has several drawbacks (no hybrid functionals, Born–Oppenheimer molecular dynamics only), but the picture obtained is clear: there is no reason to assume that nuclei do anything strange during photoreactions. The Born–Oppenheimer approximation breaks down, but we make no use of the Born–Oppenheimer approximation. In particular, we make no product ansatz, assigning an extended wave function to the nuclei. The nuclei move as point particles in the field generated by the electrons. There is no nuclear entanglement and no need for a measurement to form the product state, and this is even true for photoreactions involving hydrogen.

For clarity, it should be mentioned that the expression "Born–Oppenheimer" is used in three different ways: we do make use of the so-called Born–Oppenheimer potential energy surfaces and of so-called Born–Oppenheimer molecular dynamics, while we do not use the Born–Oppenheimer approximation. Born–Oppenheimer potential energy surfaces always contain the nuclear–nuclear interaction, which is not the case for the

electronic Hamiltonian generated within the Born–Oppenheimer approximation. Likewise, to perform Born–Oppenheimer molecular dynamics simulations on these surfaces, no use of the Born–Oppenheimer approximation is needed. To derive BOMD, it makes more sense to start from the Car–Parrinello Lagrangian and to set the fictitious electron mass to zero. Thanks to the heroic implementations of Roberto Car and Michele Parrinello, and, a bit later, of Jürg Hutter, many-particle Newton theory is available in AIMD codes and works perfectly. Comparison to experiment yields no hint as to how to improve the classical treatment of nuclear motion. Note, however, that we have not yet investigated and understood all relevant phenomena, in particular, low-temperature heat capacities and phase transitions. In single studies, we were successful [1,37], but we do not yet have a complete picture due to the limitations of practical calculations.

Supplementary Materials: The following supporting information can be downloaded at: https://www.mdpi.com/article/10.3390/hydrogen4010002/s1, Figures S1–S5: Stability tests. Figure S6: Energies during the photodissociation of phenol, BOMD simulation. Figure S7: Energies during the photoisomerization of [2,2′-bipyridyl]-3,3′-diol, BOMD simulation. Figure S8: Energies during the photodissociation of [2,2′-bipyridyl]-3,3′-diol, CPMD simulation.

Data Availability Statement: Input files for CPMD version 4.3 and corresponding output files are available on demand from the corresponding author.

Conflicts of Interest: The author declares no conflict of interest.

Abbreviations

The following abbreviations are used in this manuscript:

AIMD	Ab initio molecular dynamics
BOMD	Born–Oppenheimer molecular dynamics
CPMD	Car–Parrinello molecular dynamics
DFT	Density functional theory
ESIPT	Excited-state intramolecular proton transfer
HOMO	Highest occupied molecular orbital
LUMO	Lowest unoccupied molecular orbital
NEO	Nuclear-electronic orbital method
QM/MM	Quantum mechanics/molecular mechanics
ROKS	Restricted open-shell Kohn–Sham theory
SCF	Self-consistent field theory
TDDFT	Time-dependent DFT

References

1. Frank, I.; Genuit, S.; Matz, F.; Oschinski, H. Ammonia, water, and hydrogen: Can nuclear motion be described classically? *Int. J. Quantum Chem.* **2020**, *120*, e26142. [CrossRef]
2. Frank, I. Classical motion of the nuclei in a molecules: A concept without alternatives. *Chem. Sel.* **2020**, *5*, 1872. [CrossRef]
3. Büchel, R.C.; Rudolph, D.A.; Frank, I. Deterministic quantum mechanics: The role of the Maxwell-Boltzmann distribution. *Int. J. Quantum Chem.* **2021**, *121*, e26555. [CrossRef]
4. Car, R.; Parrinello, M. Unified Approach for Molecular Dynamics and Density-Functional Theory. *Phys. Rev. Lett.* **1985**, *55*, 2471–2474. [CrossRef] [PubMed]
5. Hutter, J.; Hutter, J.; Alavi, A.; Deutsch, T.; Bernasconi, M.; Goedecker, S.; Marx, D.; Tuckerman, M.; Parrinello, M. Version 4.3, Copyright IBM Corp 1990–2015, Copyright MPI für Festkörperforschung Stuttgart 1997–2001. Available online: http://www.cpmd.org/ (accessed on 22 October 2022).
6. Marx, D.; Parrinello, M. Ab initio path-integral molecular dynamics. *Z. Phys. B* **1994**, *95*, 143. [CrossRef]
7. Marx, D.; Parrinello, M. Structural quantum effects and three-centre two-electron bonding in CH_5^+. *Nature* **1995**, *375*, 216. [CrossRef]
8. Marx, D.; Parrinello, M. Ab initio path-integral molecular dynamics: Basic ideas. *J. Chem. Phys.* **1996**, *104*, 4077. [CrossRef]
9. Marx, D.; Parrinello, M. The effect of quantum and thermal fluctuations on the structure of the floppy molecule $C_2H_3^+$. *Science* **1996**, *271*, 179. [CrossRef]

10. Lan, Z.; Domcke, W.; Vallet, V.; Sobolewski, A.L.; Mahapatra, S. Time-dependent quantum wave-packet description of the $^1\pi\sigma^*$ photochemistry of phenol. *J. Chem. Phys.* **2005**, *122*, 224315. [CrossRef]

11. Domcke, W.; Yarkony, D.R. Role of Conical Intersections in Molecular Spectroscopy and Photoinduced Chemical Dynamics. *Annu. Rev. Phys. Chem.* **2012**, *63*, 325. [CrossRef]

12. Ramesh, S.G.; Domcke, W. A multi-sheeted three-dimensional potential-energy surface for the H-atom photodissociation of phenol. *Faraday Discuss.* **2013**, *163*, 73. [CrossRef]

13. Xie, W.; Domcke, W. Accuracy of trajectory surface-hopping methods: Test for a two-dimensional model of the photodissociation of phenol. *J. Chem. Phys.* **2017**, *147*, 184114. [CrossRef]

14. Webb, S.P.; Iordanov, T.; Hammes-Schiffer, S. Multiconfigurational nuclear-electronic orbital approach: Incorporation of nuclear quantum effects in electronic structure calculations. *J. Chem. Phys.* **2002**, *117*, 4106. [CrossRef]

15. Ben-Nun, M.; Quenneville, J.; Martinez, T. Ab Initio Multiple Spawning: Photochemistry from First Principles Quantum Molecular Dynamics. *J. Phys. Chem. A* **2000**, *104*, 5161. [CrossRef]

16. Curchod, B.F.E.; Martinez, T.J. Ab Initio Nonadiabatic Quantum Molecular Dynamics. *Chem. Rev.* **2018**, *118*, 3305. [CrossRef]

17. Frank, I.; Hutter, J.; Marx, D.; Parrinello, M. Molecular dynamics in low-spin excited states. *J. Chem. Phys.* **1998**, *108*, 4060. [CrossRef]

18. Tavernelli, I.; Röhrig, U.; Roethlisberger, U. Molecular dynamics in electronically excited states using time-dependent density functional theory. *Mol. Phys.* **2005**, *103*, 963. [CrossRef]

19. Alonso, J.L.; Andrade, X.; Echenique, P.; Falceto, F.; Prada-Gracia, D.; Rubio, A. Efficient Formalism for Large-Scale Ab Initio Molecular Dynamics based on Time-Dependent Density Functional Theory. *Phys. Rev. Lett.* **2008**, *101*, 096403. [CrossRef]

20. Lopata, K.; Govind, N. Modelling Fast Electron Dynamics with Real-Time Time-Dependent Density Functional Theory: Application to Small Molecules and Chromophores. *J. Chem. Theory Comput.* **2011**, *7*, 1344. [CrossRef]

21. Lian, C.; Hu, S.Q.; Guan, M.X.; Meng, S. Momentum-resolved TDDFT algorithm in atomic basis for real time tracking of electronic excitation. *J. Chem. Phys.* **2018**, *149*, 154104. [CrossRef]

22. Lian, C.; Ali, Z.A.; Kwon, H.; Wong, B.M. Indirect but Efficient: Laser-Excited Electrons Can Drive Ultrafast Polarization Switching in Ferroelectroc Materials. *J. Phys. Chem. Lett.* **2019**, *10*, 3402. [CrossRef] [PubMed]

23. Marx, D.; Hutter, J. *Ab Initio Molecular Dynamics: Basic Theory and Advanced Methods*; Cambridge University Press: Cambridge, UK, 2009.

24. Grimme, S. Semiempirical GGA-type density functional constructed with a long-range dispersion correction. *J. Comput. Chem.* **2006**, *27*, 1787–1799. [CrossRef] [PubMed]

25. Troullier, N.; Martins, J.L. Efficient Pseudopotentials for Plane-Wave Calculations. *Phys. Rev. B* **1991**, *43*, 1993. [CrossRef] [PubMed]

26. Boero, M.; Parrinello, M.; Terakura, K.; Weiss, H. Car-Parrinello study of Ziegler-Natta heterogeneous catalysis: Stability and destabilization problems of the active site models. *Mol. Phys.* **2002**, *100*, 2935–2940. [CrossRef]

27. Bernardi, F.; Olivucci, M.; Robb, M.A. Potential energy surface crossings in organic photochemistry. *Chem. Soc. Rev.* **1996**, *25*, 321. [CrossRef]

28. Nonnenberg, C.; Grimm, S.; Frank, I. Restricted open-shell Kohn-Sham theory for $\pi - \pi^*$ transitions. II. Simulation of photochemical reactions. *J. Chem. Phys.* **2003**, *119*, 11585. [CrossRef]

29. Frank, I.; Damianos, K. Restricted Open-Shell Kohn-Sham Theory: Simulation of the Pyrrole Photodissociation. *J. Chem. Phys.* **2007**, *126*, 125105. [CrossRef]

30. Shu, Y.; Truhlar, D.G. Diabatization by machine intelligence. *J. Chem. Theory Comput.* **2020**, *16*, 6456. [CrossRef]

31. Sobolewski, A.L.; Domcke, W. Photoinduced Electron and Proton Transfer in Phenol and Its Clusters with Water and Ammonia. *J. Phys. Chem. A* **2001**, *105*, 9275. [CrossRef]

32. Ben-Nun, M.; Molnar, F.; Lu, H.; Phillips, J.C.; Martinez, T.J.; Schulten, K. Quantum dynamics of the femtosecond photoisomerization of retinal in bacteriorhodopsin. *Faraday Discuss.* **1998**, *110*, 447. [CrossRef]

33. Röhrig, U.; Guidoni, L.; Laio, A.; Frank, I.; Röthlisberger, U. A molecular spring for vision. *J. Am. Chem. Soc.* **2004**, *126*, 15328. [CrossRef]

34. Feynman, R.P.; Leighton, R.B.; Sands, M. *The Feynman Lectures on Physics*, 2nd ed.; Pearson Education: London, UK; California Institute of Technology: Pasadena, CA, USA, 2006.

35. Yu, Q.; Pavosevic, F.; Hammes-Schiffer, S. Development of nuclear basis sets for multicomponent quantum chemistry methods. *J. Chem. Phys.* **2020**, *152*, 244123. [CrossRef]

36. Tao, Z.; Roy, S.; Schneider, P.E.; Pavosevic, F.; Hammes-Schiffer, S. Analytical Gradients for Nuclear–Electronic Orbital Time-Dependent Density Functional Theory: Excited-State Geometry Optimizations and Adiabatic Excitation Energies. *J. Chem. Theory Comput.* **2021**, *17*, 5110. [CrossRef]

37. Rohloff, E.; Rudolph, D.A.; Strolka, O. Classical nuclear motion: Does it fail to explain reactions and spectra in certain cases? *Int. J. Quantum Chem.* **2022**, *122*, e26902. [CrossRef]